Publications of the Korean Astronomical Society
30: 423 ∼ 427, 2015 September

pISSN: 1225-1534
eISSN: 2287-6936
http://dx.doi.org/10.5303/PKAS.2015.30.2.423

ACTIVE GALACTIC NUCLEUS INTERACTION WITH THE HOT GAS ENVIRONMENT: UNDERSTANDING FROM THE RADIO AND X-RAY DATA

Dharam V. Lal
National Centre for Radio Astrophysics (TIFR), Pune University Campus, Ganeshkhind P.O., Pune 411 007, India
E-mail: dharam@ncra.tifr.res.in
(Received November 30, 2014; Reviced May 31, 2015; Aaccepted June 30, 2015)

ABSTRACT

Recognition of the role of radio galaxies in the universe has been increasing in recent years. Their colossal energy output over huge volumes is now widely believed to play a key role not only in the formation of galaxies and their supermassive black holes, but also in the evolution of clusters of galaxies and, possibly, the cosmic web itself. In this regard, we need to understand the inflation of radio bubbles in the hot gas atmospheres of clusters and the importance of the role that radio galaxies play in the overall energy budget of the intracluster medium. Here, we present results from X-ray and radio band observations of the hot gas atmospheres of powerful, nearby radio galaxies in poor clusters.

Key words: galaxies: individual (3C 31, 3C 270.1, 3C 449) – hydrodynamics – intergalactic medium – X-rays: galaxies: clusters

1. INTRODUCTION

All galaxies and quasars appear to be sources of radio emission at some level. Normal spiral galaxies such as our own galactic system are near the low end of the radio luminosity function and have radio luminosities near 10^{37} erg s^{-1}. Some Seyfert galaxies, starburst galaxies, and the nuclei of active elliptical galaxies are 100 to 10^3 times more luminous. Radio galaxies (and some quasars), where the radio emission is powered by active galactic nucleus (AGN) activity rather than star formation, are powerful radio sources at the high end of the luminosity function with radio band luminosities up to 10^{45} erg s^{-1} (Peterson, 1997).

Extended radio galaxies constitute the largest known physical structures in the universe. Their energy content is very large, $\simeq 10^{60}$ erg. Several attempts at understanding the origin of this (accretion) energy and the manner in which it is converted into relativistic particles and magnetic fields have been made, including the 'spin paradigm' (Blandford & Znajek 1977). High-resolution radio images generally show a very compact component which is coincident with an AGN, called the 'central engine'. Long collimated 'jets' extend away from the compact central core toward the outer radio lobes; in some sources these jets eventually end up terminating at 'hotspots'. The primary observables for a radio galaxy at a known redshift are, for the purpose of this article, to be regarded as the morphology and the luminosity at some common rest frame frequency derived from the spectral shape and the redshift in some chosen cosmological model.

The study of radio galaxies has evolved somewhat unsystematically, *e.g.*, complex classification schemes, objects which were once thought to be different are now being found to be related, etc. Attempts at morphological classification and statistical studies include 'head-tail radio galaxies' – (Miley et al. 1972, Fanaroff & Riley 1974) a classification scheme for strong and weak radio galaxies with powerful, edge-brightened (with highly collimated jets and compact 'hotspots') structure and less powerful, centre-brightened structure (with less collimated jets), respectively, being FR class I and class II radio galaxies.

1.1. Low-/High-excitation Radio Galaxies

In addition, with the advent of detailed X-ray observations using *Chandra* and *XMM-Newton*, and well established optical surveys, clear evidence for a fundamental dichotomy related to the accretion onto the central supermassive black hole, called 'high-excitation' and 'low-excitation' modes, is also seen. Briefly, Table 1 (reproduced from Garofalo, Evans & Sambruna 2010) summarises the broad properties of low- and high-excitation radio galaxies.

1.2. Emission Processes

The energetics of radio sources are important not only because of their relation to the emission process but because they also play an important role in all considerations of how radio sources are held together or confined.

The emission in the radio band from radio galaxies is synchrotron emission, as inferred from its very

Table 1
Overview of the properties of low- and high-excitation radio galaxies (Reproduced from Garofalo, Evans, Sambruna 2010).

	Low-excitation radio galaxy (LERG)	High-excitation radio galaxy (HERG)
Definition	No narrow optical line emission.	Prominent optical emission lines, either narrow (NLRG) or broad (BLRG), or quasar.
FR classification	Almost all FR Is are LERGs at z=0. Significant population of FR IIs at $z \sim$0.5.	Most FR IIs are HERGs, as are a handful of FR Is (e.g., Cen A).
X-ray spectra	Jet-related unabsorbed power law only. Upper limits only to 'hidden' accretion-related emission.	Jet-related unabsorbed power law + significant accretion contribution (heavily absorbed in NLRGs).
Accretion-flow type	Highly sub-Eddington. Likely radiatively inefficient.	Reasonable fraction of Eddington. Likely standard accretion disk.
Optical constraints	Strong radio/optical/soft X-ray correlations. Optical emission is jet-related.	Strong radio/optical/soft X-ray correlations. Optical emission is jet-related.

smooth, broad-band nature and strong polarization. In the X-ray band, the population of relativistic electrons that gives rise to the radio emission can also produce X-rays. There are two methods: 1) the synchrotron process and 2) the inverse-Compton process. The former simply states that the synchrotron process produces not only radio emission, but also X-ray emission. In the latter, the relativistic electrons in the radio lobes, via. inverse-Compton process, scatter the cosmic microwave background (CMB) photons with frequency $\nu \sim 10^{11}(1+z)$ (z is redshift) and boost them up to a frequency $\nu_{\rm inverse-Compton} \sim \gamma^2\nu$ (where γ is the Lorentz factor), *i.e.*, into the X-ray and gamma-ray regions. Since the CMB energy density $u_{\rm CMB} = 4.1 \times 10^{-13}(1+z)^4$ ergs s^{-1} is precisely known, a comparison of the synchrotron radio emission and the inverse-Compton X-ray flux give estimates of energy densities in the magnetic field in radio lobes and lets us examine energy equipartition between particles and fields.

High resolution imaging using *Chandra* has shown X-ray emission from the jets of radio galaxies, which is interpreted as synchrotron emission. Synchrotron emission is often observed from jets of weak radio galaxies, such as Centaurus A (Hardcastle et al., 2007) and M 87 (Perlman & Wilson, 2005), as well as from some terminal hotspots in powerful radio galaxies (Hardcastle et al., 2007). Similarly, *Chandra* has also shown that the hotspots of several radio galaxies, e.g. Cygnus A, while undetected at optical wavelengths, radiate significantly in the X-ray (Wilson et al., 2000), which is interpreted as evidence that some hotspots emit X-rays by a synchrotron self-Compton process. Finally, extended X-ray emission from the radio lobes of powerful, FR II radio galaxies and quasars is thought to be produced by inverse-Compton scattering off the CMB (Feigelson et al., 1995; Hardcastle et al., 2002a, 2005).

2. RADIO AND X-RAY STUDY OF RADIO GALAXIES

Therefore, X-ray observations of radio galaxies can provide important clues about the dynamics and particle acceleration in the relativistic jets and outflows. Or in other words, X-ray imaging has opened new vistas on the structure and evolution of groups and clusters and their member galaxies. The aim of this paper is to provide three examples to understand the nature of X-ray emission from three parts of radio galaxies. These three aspects reviewed in this contribution are

- the nature of X-ray emission from a radio jet close to the core of the weak FR I, 3C 31 radio galaxy (Hardcastle et al., 2002b; Lanz et al., 2011),
- the nature of X-ray emission from the radio lobes of the strong FR II radio galaxy, 3C 270.1 (Wilkes et al., 2012) and
- the nature of the hot gas around the canonical FR I radio galaxy 3C 449 (Lal et al., 2013).

3. RADIO GALAXY

3.1. Jet Emission

Our first example is a case study of 3C 31. It is a nearby twin-jet radio source hosted within the early-type galaxy NGC 383 at a redshift of 0.0168. The twin jets are aligned roughly along a north-south axis. The northern jet is straight, narrow and brighter in the central 20 kpc, beyond this distance the jet flares. We clearly detect X-ray emission using *Chandra*, from the jet component close to the radio core in 3C 31. The presence of X-ray emission suggests that there is on-going particle acceleration in these regions. Often radio, infrared, optical, and X-ray emission from FR I jets can be modeled as synchrotron emission from a single electron energy distribution described by a broken power law. In this example, we model the broadband spectra of 3C 31 with clearly measured jet flux densities in radio, infrared, optical and X-ray in the region closest to the nucleus (please refer Figure 4 of Lanz et al. 2011). The broken power-law model of synchrotron emission from a broken power-law electron energy distribution gives an acceptable fit to the data. Therefore, here again, radio through X-ray spectra in these regions demonstrate that the emission, which can be interpreted as synchrotron emission from a broken power-law distribution of electron energies (Hardcastle et al. 2002b; Lanz et al. 2011).

3.2. Radio Lobe Emission

The radio galaxy 3C 270.1 at a redshift of 1.532 has the double-lobed radio structure characteristic of FR II. We model the unperturbed, static and weak but significant X-ray emission associated with the southeastern extension of the northern radio lobe, called the 'N-C-jet-bend' feature (please refer Figure 1 of Wilkes et al., 2012) detected using *Chandra*. The emission can be explained by the predictions of inverse-Compton scattering of CMB photons, can be brought into agreement with the observations if the magnetic field is 3 $\pm$1 nT. This field is a factor of $\sim$7–10 lower than the equipartition magnetic field, which is a larger than departure (Croston et al., 2005).

Here, one should note that the low energy end of the spectrum of the relativistic particles in radio galaxies is essentially unconstrained. This is true for the 3C 270.1 radio source and other sources in general, and the effect is more severe for high-redshift radio galaxies than for low-redshift radio galaxies. In the example presented above, the electron energy required to scatter a photon to X-ray energies depends on the initial energy of the photon: if the photon is one of the radio photons emitted by the electron population itself, then Lorentz factors of 10^4 are required, whereas if the photon comes from the all-pervading CMB radiation, Lorentz factors of 10^3 are required. The key fact about the inverse-Compton process is that the energy radiated in scattered photons (for a given electron and photon energy) is the product of the number density of electrons and photons, hence, the observations of inverse-Compton emission are always combined with the constraints from the synchrotron emission. However, it is difficult to constrain the synchrotron emission for Lorentz factors below 100–10^3 and often one is forced to make assumptions, *e.g.* a flattening or a low energy cut-off in the spectrum at these energies.

3.3. Radio Galaxy Interaction with the Hot Gas Environment

Although X-ray observations of several radio galaxies exists in a variety of environments including cluster outskirts and the field, here we present an example of the canonical FR I radio galaxy 3C 449. 3C 449 exhibits a complex radio morphology on spatial scales from parsecs to hundreds of kiloparsecs. The source is characterised by an unresolved core, two symmetrically opposed jets, and very extended radio lobes. Each jet is remarkably straight from the nucleus before deviating sharply towards the west, dropping in surface brightness and terminating in large diffuse radio lobes. Since both jets bend in the same direction, rotation effects cannot cause this morphology (Birkinshaw et al., 1981).

Several panels in Figure 1 show following features:

- There is an elongated diffuse structure extending $\simeq$110 kpc to the northeast of the core, labeled 'cool-filament'.
- There are two arc-shaped tangential edges in the surface brightness $\simeq$33 kpc to the southeast and to the west of the core.
- There is an X-ray cavity, i.e. a decrement in X-ray emission, at the location of the southern inner radio lobe. This cavity is surrounded by a rim of enhanced brightness.
- There is a tunnel-like feature in the X-ray emission connecting the southern cavity and the group core, marked with a dashed line, which coincides with the southern radio jet.

We further discuss one key feature, the presence of surface brightness edges mentioned above. A careful treatment of each of these surface brightness discontinuities suggests that the gas temperature and density change discontinuously but the pressure typically remains at or near equilibrium across the front, hence, these are probably sloshing cold fronts due to a merger (Lal et al., 2013). Additionally, the straight inner jet flares at approximately the position where it crosses the contact edge, suggesting that the jet is entraining and thermalising some of the hot gas as it crosses the edge. This is consistent with hydrodynamic simulations of jets crossing density discontinuities with shear flow which show that well collimated jets can become partially disrupted (Loken et al., 1995); the disruption of the jets of 3C 449 by this type of edge was first predicted by Katz-Stone & Rudnick (1997). It is therefore not unreasonable to interpret the fact that jets crossing density edges can become partially disrupted and inflate to form inner radio lobes as a consequence of observed signatures of interactions between an AGN and its surrounding medium (Lal et al., 2013).

4. LOOKING AHEAD

The statistics, *i.e.* general conclusions about the population as a whole are already available in the literature from optical surveys and also to a large extent from radio surveys, essentially only at these two key wavebands. This approach of drawing general conclusions about the population as a whole is lacking in the X-ray band. Some of the results presented here are primarily from the published results of observations of interesting individual objects.

In the meantime, hopefully, the low-frequency array (LOFAR), which is already making enormous progress, is expected to provide a major step in our understanding of the physics of radio sources. LOFAR will reach unprecedented sensitivities and resolution in the frequency range 40-240 MHz and this will immediately allow us to study the electron spectrum of Lorentz factors of $\sim 10^3$, as discussed in Sec. 3.2. This is an appreciable step forward, however it is still not enough to catch the bulk of the particle energy in radio sources and to constrain the physics of particle acceleration in these sources. Furthermore, in terms of current X-ray observing facilities, *Chandra* and *XMM-Newton* will not last for ever, their immediate replacements, including *Athena*[1] and *SMART-X*[2] though they are still at the design stage, may become a reality before current facilities fade away. It thus seems that the future is bright, and radio and

[1] https://www.mpe.mpg.de/Athena
[2] http://smart-x.cfa.harvard.edu/index.html

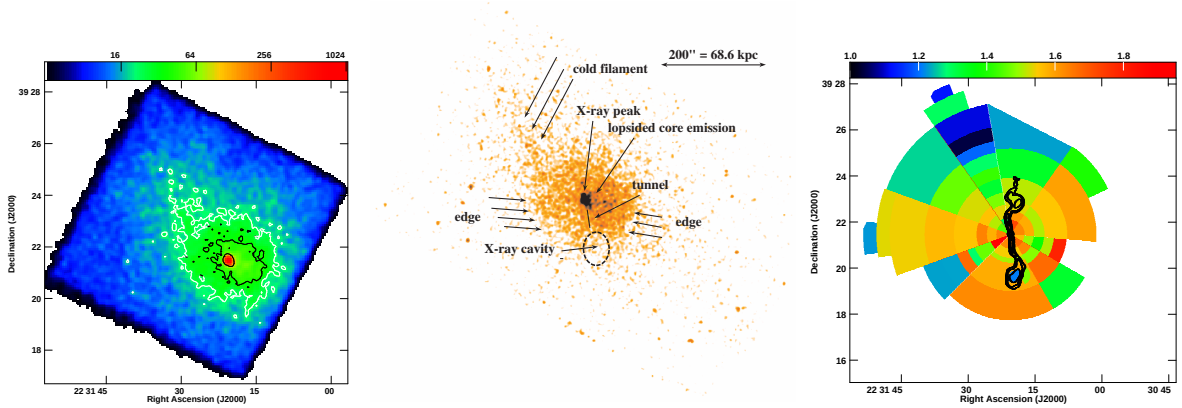

Figure 1. Left panel: Combined *Chandra*/ACIS-S counts image of 3C 449 in the 0.5–2.0 kilo-electronvolt (keV) band. The image is binned to 4″ pixels and smoothed with a Gaussian ($\sigma = 6''$). All point sources, other than the active nucleus of 3C 449, have been removed. We see diffuse thermal emission in the soft band extending over the entire field of view, 12′ (≃240 kpc) along the east-west axis (Lal et al 2013). Middle panel: Background-subtracted, exposure-corrected, Gaussian-smoothed ($\sigma = 4''$) *Chandra* image in the energy range 0.5–2.0 keV. Features of interest are labeled including lopsided gas emission near core, the cool filament, the eastern and western edges, the cavity associated with the southern inner radio lobe, and the tunnel associated with the southern inner jet. Right panel: Projected thermodynamic temperature map using the merged data. The temperature map has radio contours overlaid. The color bar gives the temperature scale in keV.

X-ray band observations will continue to play an important role for radio galaxies.

ACKNOWLEDGMENTS

The APRIM Deajeon meeting was excellent and I would like to thank all those involved in organising it. I would also like to thank R.P. Kraft, M.J. Hardcastle and W.R. Forman and last, but certainly not least, A.P. Rao and S. Bhatnagar, my mentors without the support of whom this journey of being in research would not have been possible. Much of the work discussed in this paper stems from collaborative research work involving the following: my mentors, and M. Birkinshaw, J.H. Croston, C. Jones-Forman, L. Lanz, P.E.J. Nulsen, B.J. Wilkes and D. Worrall. The scientific results reported in this article are based to a significant degree on observations made by the *Chandra* X-ray Observatory by the PI team R.P. Kraft, M.J. Hardcastle, B.J. Wilkes, W.R. Forman and published previously in cited articles. This research has made use of the NASA/IPAC Extragalactic Database (NED) which is operated by the Jet Propulsion Laboratory, California Institute of Technology, under contract with NASA. This research has made use of NASA's Astrophysics Data System.

REFERENCES

Birkinshaw, M., Laing, R. A., & Peacock, J. A., 1981, Radio Synthesis Observations of 3C 296, 3C 442A and 3C 449 at 0.4, 1.4 and 2.7 GHz, MNRAS, 197, 253

Blandford, R. D. & Znajek, R. L., 1977, Electromagnetic Extraction of Energy from Kerr Black Holes, MNRAS, 179, 433

Croston, J. H., Hardcastle, M. J., & Harris, D. E., et al., 2005, An X-Ray Study of Magnetic Field Strengths and Particle Content in the Lobes of FR II Radio Sources, ApJ, 626, 733

Fanaroff, B. L. & Riley, J. M., 1974, The Morphology of Extragalactic Radio Sources of High and Low Luminosity, MNRAS, 167, P31

Feigelson E. D., Laurent-Muehleisen, S. A., Kollgaard, R. I., & Fomalont, E. B., 1995, Discovery of Inverse-Compton X-Rays in Radio Lobes, ApJ, 449, L149

Garofalo, D., Evans, D. A., & Sambruna, R. M., 2010, The Evolution of Radio-Loud Active Galactic Nuclei as a Function of Black Hole Spin, MNRAS, 406, 975

Hardcastle M. J., Birkinshaw M., Cameron R., Harris D. E., Looney L.W., & Worrall D. M., 2002a, Magnetic Field strengths in the Hotspots and Lobes of Three Powerful FRII Radio Sources, ApJ, 581, 948

Hardcastle M. J., Worrall, D. M., Birkinshaw M., Laing, R. A., & Bridle, A. H., 2002b, A Chandra Observation of the X-ray Environment and Jet of 3C 31, MNRAS, 334, 182

Hardcastle, M. J., 2005, Jets, Hotspots and Lobes: What X-ray Observations Tell us about Extragalactic Radio Sources, Phil. Trans. R. S. A, 363, 2711

Hardcastle, M. J. Kraft, R. P., & Sivakoff, G. R., et al., 2007, New Results on Particle Acceleration in the Centaurus A Jet and Counterjet from a Deep Chandra Observation, ApJ, 670, L81

Katz-Stone, D. M & Rudnick, L., 1997, An Analysis of the Synchrotron Spectrum in the Fanaroff-Riley Type I Galaxy 3C 449, ApJ, 488, 146

Lal, D.V., Kraft, R. P., & Randall, S. W., et al., 2013, Gas Sloshing and Radio Galaxy Dynamics in the Core of the 3C 449 Group, ApJ, 764, 83

Lanz, L., Bliss, A., Kraft, R. P., Birkinshaw, M., & Lal, D. V., et al., 2011, The Infrared Jet in 3C 31, ApJ, 731, L52

Loken, C., Roettiger, K., Burns, J. O., & Norman, M., 1995, Radio Jet Propagation and Wide-Angle Tailed Radio Sources in Merging Galaxy Cluster Environments, ApJ, 445, 80

Miley, G. K., Perola, G. C., van der Kruit, P. C., & van der Laan, H., 1972, Active Galaxies with Radio Trails in Clusters, Nature, 237, 269

Perlman, E. S. & Wilson, A. S., 2005, The X-Ray Emissions from the M87 Jet: Diagnostics and Physical Interpretation, ApJ, 627, 140

Peterson, B. M., 1997, An Introduction to Active Galactic Nuclei, Cambridge: Cambridge University Press
Wilkes, B. J., Lal, D. V., & Worrall, D. M., et al., 2012, Chandra X-Ray Observations of the Redshift 1.53 Radio-loud Quasar 3C 270.1, ApJ, 745, 84
Wilson, A. S, Young, A. J., & Shopbell, P. L., 2000, Chandra Observations of Cygnus A: Magnetic Field Strengths in the Hot Spots of a Radio Galaxy, ApJ, 544, L27